Three-dimensional brain growth abnormalities in childhood-onset schizophrenia visualized by using tensor-based morphometry

Nitin Gogtay*†‡, Allen Lu†§, Alex D. Leow§¶, Andrea D. Klunder§, Agatha D. Lee§, Alex Chavez*, Deanna Greenstein*, Jay N. Giedd*, Arthur W. Toga§, Judith L. Rapoport*, and Paul M. Thompson§

*Child Psychiatry Branch, National Institute of Mental Health, Bethesda, MD 20892; and §Laboratory of Neuro Imaging and ¶Semel Institute for Neuroscience, University of California School of Medicine, Los Angeles, CA 90095

Earlier studies revealed progressive cortical gray matter (GM) loss in childhood-onset schizophrenia (COS) across both lateral and medial surfaces of the developing brain. Here, we use tensor-based morphometry to visualize white matter (WM) growth abnormalities in COS throughout the brain. Using high-dimensional elastic image registration, we compared 3D maps of local WM growth rates in COS patients and healthy children over a 5-year period, based on analyzing longitudinal brain MRIs from 12 COS patients and 12 healthy controls matched for age, gender, and scan interval. COS patients showed up to 2.2% slower growth rates per year than healthy controls in WM ($P = 0.02$, all P values corrected). The greatest differences were in the right hemisphere ($P = 0.006$). This asymmetry was attributable to a right slower than left hemisphere growth rate mapped in COS patients ($P = 0.037$) but not in healthy controls. WM growth rates reached 2.6% per year in healthy controls ($P = 0.0002$). COS patients showed only a 1.3% per year trend for growth in the left hemisphere ($P = 0.066$). In COS, WM growth rates were associated with improvement in the Children's Global Assessment Scale ($R = 0.64$, $P = 0.029$). Growth rates were reduced throughout the brain in COS, but this process appeared to progress in a front-to-back (frontal-parietal) fashion, and this effect was not attributable to lower IQ. Growth rates were correlated with functional prognosis and were visualized as detailed 3D maps. Finally, these findings also confirm that the progressive GM deficits seen in schizophrenia are not the result of WM overgrowth.

development | imaging | MRI | white matter

Childhood-onset schizophrenia (COS) is a disabling neuropsychiatric disorder characterized by psychotic symptoms, sensory disturbances, social withdrawal, and inappropriate or flattened effect. Schizophrenia is rare in children, and COS, defined by onset of psychotic symptoms before age 13, is neurobiologically continuous but a clinically more severe form of the adult disorder with more severe premorbid symptoms and poorer prognosis (1, 2). The cause of schizophrenia is unknown, but is increasingly considered to be a neurodevelopmental disorder with a strong genetic predisposition (1, 3–5).

Earlier studies revealed a dynamically spreading wave of accelerated cortical gray matter (GM) loss in COS patients (2, 6, 7) and progressive ventricular expansion and hippocampal volume loss (8, 9). We found that the GM loss in COS started in parietal cortices and proceeded frontally to envelop dorsolateral prefrontal and temporal cortices including the superior temporal gyrus during adolescent years (7). As COS patients matured into young adults, this GM loss gradually merged into the adult pattern of localization with deficits in prefrontal and superior temporal cortices, suggesting a neurobiological continuity between COS and adult-onset schizophrenia (AOS) (2). Studies of monozygotic twins discordant for schizophrenia (4) and our recent longitudinal studies in healthy full siblings of COS patients (10) have suggested that these deficits are genetically influenced in prefrontal and temporal cortices whereas the parietal deficits may have a nongenetic trigger.

Dynamic cortical maps have helped chart the anatomical sequence of normal (11) and abnormal (7, 12) GM development, but few studies have assessed growth rates in the white matter (WM). Recently, a cross-sectional study of 24 healthy adolescent males showed continued maturational changes, particularly in the arcuate fasciculus by using diffusion tensor imaging (DTI) (13), and a small longitudinal study, designed mainly to validate tensor-based morphometry (TBM) for detecting brain growth patterns, showed lobar WM growth across the cerebrum (14).

It has been debated whether GM deficits observed in schizophrenia, in structural MRI scans, may just reflect WM encroachment. Independent measures of WM growth could help address this question. The integrity of WM is also of interest to determine whether the abnormalities in COS are primarily cortical, or whether they affect tissue growth rates throughout the brain. Fewer studies have examined WM alterations in COS, but progressive reductions have been observed in the splenium of the corpus callosum (15). A recent cross-sectional study of 26 patients with adolescent-onset schizophrenia suggested that the structural integrity of WM tracts was disrupted in the anterior cingulate region (16). However, there are no studies showing detailed 3D maps of growth pattern abnormalities in schizophrenia throughout the brain, which would serve to indicate brain regions that are affected in the illness and may offer additional surrogate markers of disease progression for clinical trials.

Here, we used the computational approach TBM to create 3D maps of local tissue growth rates in patients and controls. This type of approach has been useful in visualizing the rates of tissue growth in the corpus callosum and basal ganglia of children scanned longitudinally (17) and has identified systematic brain tissue changes in groups of subjects (18). By comparing patients with controls at baseline and follow-up, we also created 3D maps to show the degree of tissue reduction in COS shortly after diagnosis and 5 years later. We assessed hemispheric asymmetries in growth rates on the growth pattern abnormalities observed in COS. Finally, we correlated local tissue growth rates with clinical assessment scores to relate brain tissue changes to functional outcomes.

Results

Disease Effects. Pervasive WM growth (percentage per year) was apparent in healthy controls (Fig. 1A) but not COS patients (Fig.

NEUROSCIENCE

Fig. 1. Tissue growth rates mapped in healthy controls and COS patients. (*A* and *B*) These maps show the average rates of tissue growth (red) and tissue loss (blue) throughout the brain in percentage per year, for healthy controls (*A*) and COS patients (*B*). (*C* and *D*) These corresponding maps show the significance of the tissue growth in *A* and *B*. For *A–D*, a sagittal section through the right hemisphere at the level of the occipital horn of the ventricles is shown (*Left*), followed by an axial section (*Center*), and another sagittal section although the left hemisphere (*Right*). Corroborating prior findings, these maps visualize the profile of growth in 3D, including

significant expansion of the WM and ventricles. Note the unexpected hemispheric asymmetry of growth rates in COS (right slower than left; $P < 0.037$), and the slower growth in COS patients versus healthy controls, throughout the WM (Fig. 2 directly assesses the significance of the group differences). TBM is not optimal for detecting cortical changes (see Discussion), so the cortical GM reductions observed here may be less accurate than those found in studies that directly model the cortex (6, 7, 28). Three-dimensional versions of these maps are obtainable as video sequences at: http://www.loni.ucla.edu/~thompson/MOVIES/GROWTH/video.html.
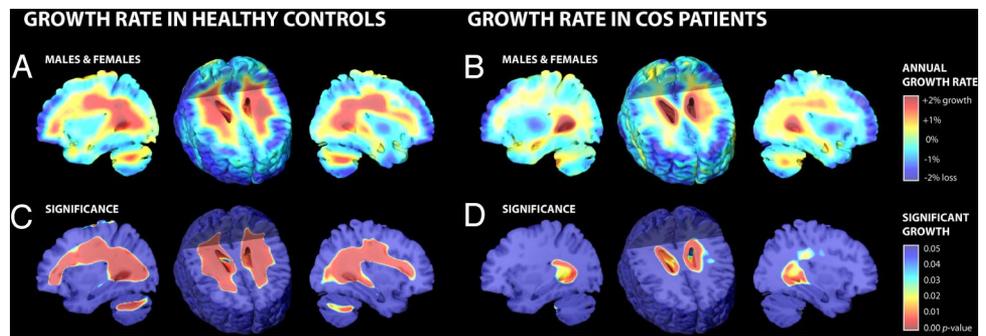
1*B*). The significance of the growth rates in each group was established by using one-sample *t* tests at each voxel (Fig. 1 *C* and *D*). Healthy controls exhibited significant growth, reaching 2.6% per year locally in WM overall (0.40 ± 0.08% growth/year, all averaged over regions of interest (ROIs); $P = 0.0002$, all P values corrected). This significant growth was detected in both left (0.41 ± 0.10% growth/year; $P = 0.0007$) and right (0.40 ± 0.09% growth/year; $P = 0.0002$) hemispheres including the left and right frontal, parietal, occipital, and temporal lobes (see Table 1). No significant growth in WM was observed for COS patients, although the left hemisphere showed a trend toward growth with local values reaching 1.2% per year (0.11 ± 0.16% growth/year; $P = 0.066$). In addition, tissue loss occurred bilaterally in the anterior cingulate region for both healthy controls (0.50 ± 0.06% loss/year; $P = 0.0001$) and COS patients (0.87 ± 0.17% loss/year; $P = 0.0001$).

A difference map shows the significantly slower WM growth rates in COS patients compared with healthy controls (Fig. 2*A*). A two-sample *t* test at each voxel (Fig. 2*B*) confirmed significantly slower tissue growth rates, up to 2.2% slower per year locally, in COS patients in WM overall (0.38% slower/year; $P = 0.020$). The disease effects were significant in the right hemisphere (0.46% slower/year; $P = 0.006$), whereas the left hemisphere showed only a trend for slower growth (0.30% slower/year; $P = 0.078$). On a lobar level, COS patients exhibited slower WM growth compared with healthy controls in the left frontal lobe and right frontal, parietal, and occipital lobes (all $P < 0.05$; see Table 1). In addition, a faster rate of tissue loss was exhibited bilaterally in the anterior

cingulate regions of COS patients compared with healthy controls (0.37% faster/year; $P = 0.025$), detected in both left (0.40% faster/year; $P = 0.047$) and right (0.35% faster/year; $P = 0.015$) hemispheres.

**Hemispheric Asymmetries in Growth.** A disease-related slowing of WM growth was significantly detected in only the right hemisphere (0.46% slower/year; $P = 0.006$), so a *post hoc* formal test for hemispheric asymmetries in growth rates was performed by using permutation testing within each subject group. A mirror image of each individual's growth rate map was created by reflecting the map with respect to its midsagittal plane. A paired two-sample *t* test, corrected for multiple comparisons, was then performed to assess whether this growth rate was significantly asymmetrical. When this test was applied to the group of healthy controls, no significant asymmetries were found, consistent with the observed symmetry in the maps (Fig. 1*A*) and with earlier maps of cortical maturation in adolescence, which follow a similar sequence in both brain hemispheres (11, 19). However, a statistically significant asymmetry for growth rates was detected in COS patients with slower WM growth in the right hemisphere compared with the left hemisphere (right slower than left, $P = 0.037$), consistent with the visual appearance of the maps (Fig. 1*B*). Perhaps because of this asymmetric WM growth in COS, and/or high variance or the limited sample size, an abnormal slowing of growth rates was detected in only the right hemisphere in COS.

Sex Differences. Because of reported sex differences in the severity or extent of anatomical deficits (20, 22), we assessed the growth

Table 1. Average tissue growth rates in healthy controls and COS patients

Region	Healthy controls		COS patients		Difference	
	Rate	P value	Rate	P value	Rate	P value
White matter overall	0.40 ± 0.08	0.0002	0.02 ± 0.15	0.100	−0.38	0.020
Left hemisphere	0.41 ± 0.10	0.0007	0.11 ± 0.16	0.066	−0.30	0.078
- Frontal lobe	0.40 ± 0.16	0.008	−0.11 ± 0.23	0.295	−0.51	0.043
- Parietal lobe	0.38 ± 0.12	0.001	0.09 ± 0.17	0.104	−0.29	0.240
- Occipital lobe	0.31 ± 0.08	0.001	0.03 ± 0.20	0.135	−0.28	0.245
- Temporal lobe	0.25 ± 0.12	0.002	0.01 ± 0.19	0.192	−0.24	0.064
Right hemisphere	0.40 ± 0.09	0.0002	−0.06 ± 0.16	0.146	−0.46	0.006
- Frontal lobe	0.29 ± 0.12	0.0004	−0.24 ± 0.26	0.580	−0.53	0.025
- Parietal lobe	0.53 ± 0.12	0.001	−0.01 ± 0.18	0.168	−0.54	0.010
- Occipital lobe	0.54 ± 0.10	0.0002	0.09 ± 0.17	0.141	−0.44	0.018
- Temporal lobe	0.03 ± 0.16	0.037	0.02 ± 0.17	0.112	−0.01	0.293
Anterior cingulate region	−0.50 ± 0.06	0.0001	−0.87 ± 0.17	0.0001	−0.37	0.025
Left hemisphere	−0.53 ± 0.08	0.0002	−0.93 ± 0.20	0.0008	−0.40	0.047
Right hemisphere	−0.48 ± 0.06	0.0003	−0.84 ± 0.16	0.0001	−0.35	0.015

Mean values for tissue growth rates (percentage per year) are shown, for healthy controls and COS patients, in specific lobar and whole-hemisphere ROIs, along with corrected P values indicating significance. Group differences in growth rate are also shown with negative rates denoting slower growth in COS patients.
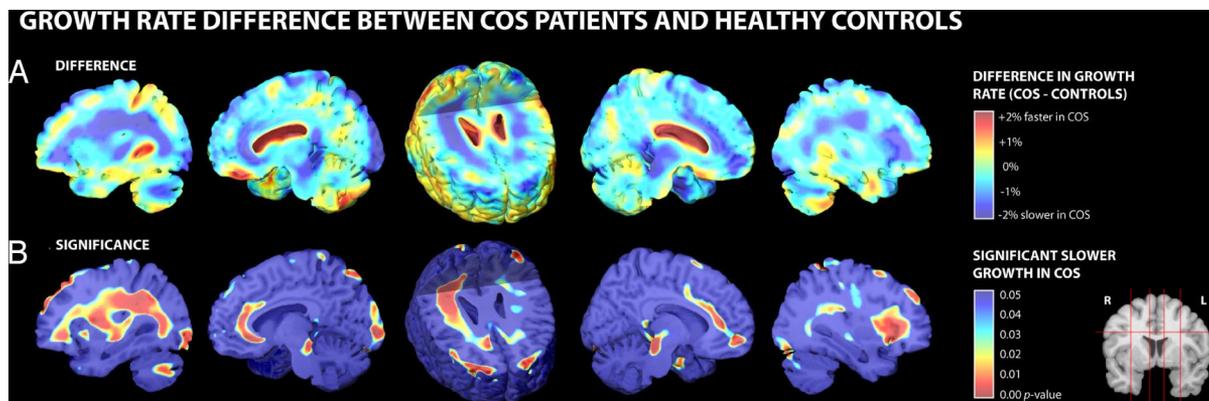
Fig. 2. Group differences in growth rates between healthy controls and COS patients. (*A*) Mean growth rates in the healthy controls are subtracted from the mean growth rates in the COS patients. There are some areas (red) where ventricular or cerebral spinal fluid space expansion is numerically greater in the COS patients, but these differences are not significant because of the large intersubject variations in these changes. (*B*) Some deep WM areas (red) show significantly slower growth in COS. Three-dimensional versions of these maps are obtainable as video sequences at: http://www.loni.ucla.edu/~thompson/MOVIES/GROWTH/video.html.

patterns by subdividing the healthy controls and COS patients into groups of males and females (Fig. 3). As observed in the combined groups, significant growth in WM overall was observed in both male (0.54 ± 0.12% growth/year; $P = 0.0001$) and female (0.27 ± 0.10% growth/year; $P = 0.0001$) healthy controls, whereas no significant growth could be detected in either male or female COS patients. Permutation testing found no significant sex differences, suggesting that slowed growth rates in COS are unrelated to sex.

Tissue Deficits at Baseline and Follow-Up. Because the dynamic maps capture local growth rates, we were concerned that deficits already present, before the baseline scan, may not have been detected in these longitudinal progression maps. To detect earlier loss, we compared tissue profiles across all 24 subjects (12 COS patients, 12 healthy controls) at their baseline and follow-up scan (Fig. 4*A*) and mapped the significance of these effects (Fig. 4*B*). To do this, a variation of the TBM method was used (22) in which all subjects were elastically deformed onto an optimized minimal deformation target (23), and the applied expansion factors were compared across groups to identify volumetric deficits or excesses.

Relative to healthy controls, COS patients exhibited deficits in WM overall reaching 14.5% locally at baseline (2.86% deficit overall; $P = 0.0004$) and reaching 15.9% locally at follow-up (3.42% deficit overall; $P = 0.001$). Similar WM deficits were detected in

both the left and right hemispheres including the frontal and parietal lobes at baseline and follow-up (all $P < 0.05$; see Table 2) with the magnitude of deficit increasing in each region. Interestingly, WM within the right parietal lobe showed only a borderline significant deficit at baseline (3.95% deficit; $P = 0.045$), but the disease effect became much greater at follow-up (5.43% deficit; $P = 0.0005$). This is consistent with the growth rate maps, where the right parietal WM showed the greatest effect size for slowed growth in COS (5.4% slower/year; $P = 0.010$). In addition, there were significant tissue deficits observed bilaterally in the anterior cingulate region at baseline (6.53% deficit; $P = 0.014$) and at follow-up (7.12% deficit; $P = 0.002$).

Correlations with Clinical Measures: Children's Global Assessment Scale (CGAS). To relate tissue growth to clinical measures, Spearman's rank test was performed to examine correlations between changes in functional CGAS scores, over time, and the local tissue growth rate. Overall, CGAS scores in COS patients improved from 28.4 ± 3.1 at baseline to 42.4 ± 5.4 at follow-up with an annualized rate of 3.4 ± 1.3 per year ($P = 0.002$).

To visualize the 3D pattern of association between change in CGAS score and local growth rates, both R values (correlation) and p values (significance) were mapped (Fig. 5 *A* and B). A positive correlation was found for the change in CGAS score with tissue growth rates for WM throughout the brain (Fig. 5C). When
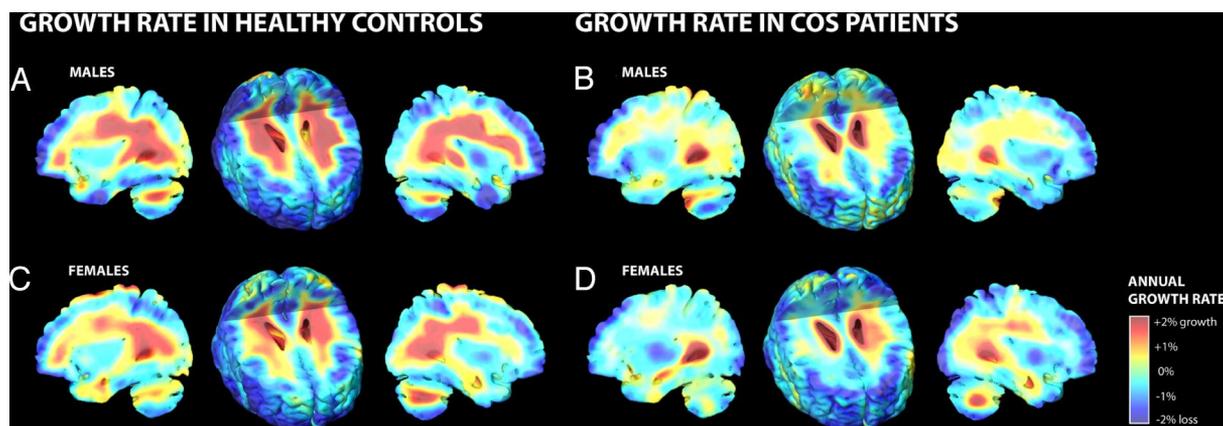
Fig. 3. Tissue growth rates mapped in males and females. Maps of tissue growth rates are shown for independent samples of male and female healthy controls (*A* and *C*) and COS patients (*B* and *D*). Similar anatomically specific profiles were observed in males (*A* and *B*) and females (*C* and *D*). A formal test of sex differences was not significant.

EARLY DEFICITS IN COS (BASELINE)   **LATE DEFICITS IN COS (FOLLOW-UP)**
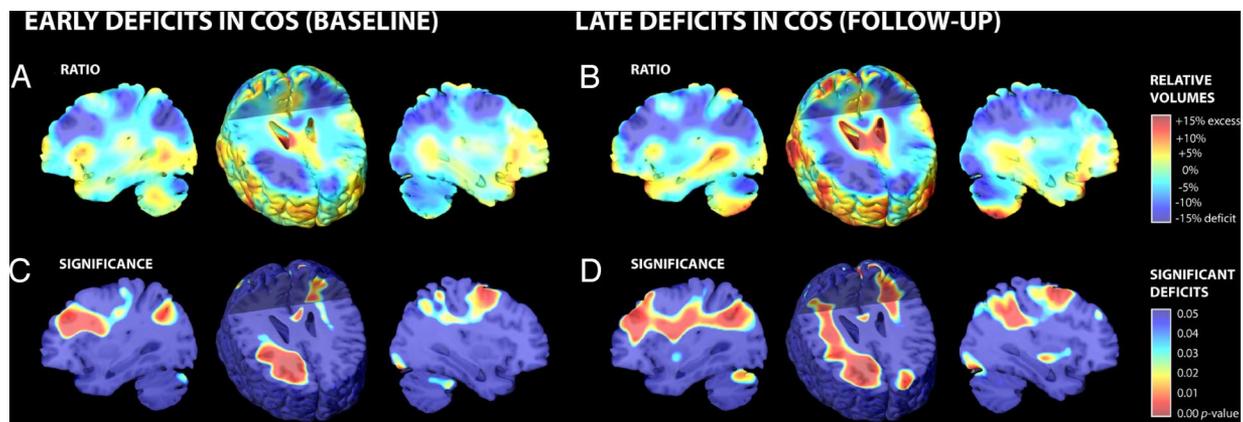
Fig. 4. Tissue deficits mapped at baseline and follow-up. (*A* and *C*) Maps of volume reductions (*A*, blue) in COS patients versus age-matched healthy controls show up to 15% volume deficits at baseline, which are significant (*C*, red). (*B* and *D*) At follow-up, a greater extent of the subcortical WM shows significant deficits in COS. This increasing deviation between COS patients and healthy controls is attributable to the partial silencing of growth rates in COS.

correlations were mapped at each point in the brain, greater improvement in clinical function was found associated with greater tissue growth in WM overall ($R = 0.64$, $P = 0.029$); this link was reproduced in both left ($R = 0.56$; $P = 0.021$) and right ($R = 0.63$; $P = 0.035$) hemispheres. On a lobar level, a highly significant correlation was detected in the left ($R = 0.66$; $P = 0.006$) and right ($R = 0.68$; $P = 0.025$) frontal lobes whereas a weak trend-level correlation was detected in the left ($R = 0.62$; $P = 0.077$) and right ($R = 0.60$; $P = 0.051$) parietal lobes. In addition, *post hoc* ROI tests also revealed similar correlations bilaterally in the anterior cingulate region ($R = 0.41$; $P = 0.048$).

Correlation with Ventricular Volume Change. Because earlier studies on COS have shown ventricular expansion, we tested the association with ventricular volume change, quantified by using automated measures (8). Correlations between the WM growth and annualized ventricular growth (change divided by time) for each group (COS and controls) were made by using the Pearson product moment correlation (*r*). For controls, correlations were $r = -0.67$, -0.58, and -0.66 (all $P < 0.05$) for total, left, and right WM growth, respectively. For COS, correlations were -0.65, -0.60, and -0.61 (all $P < 0.05$) for total, left, and right WM growth, respectively. As expected, the ventricular expansion was negatively correlated with

WM growth for both groups. However, the correlations for controls and COS were similar, suggesting that ventricular growth in COS is not differentially related to the WM growth.

Discussion

Here, we report a detailed 3D profile of tissue growth rates throughout the brain in COS. There are several main findings. First, by using this automated mapping approach, pervasive WM growth was detected in healthy controls. Peak growth rates, locally as high as 2.6% per year, contrasted with a somewhat lower mean annual rate of 0.4% growth if whole lobe or whole-hemisphere regions were considered. Second, the growth pattern in COS was almost entirely silenced, with only a trend for growth in left hemispheric WM. Growth rates in COS patients were slowed by up to 2.2% per year locally when compared with healthy controls, and the process of WM growth lag appeared to progress in a frontal-parietal direction. The WM growth rates in COS were associated with functional recovery, and finally, reduced WM growth in COS also confirms that the observed GM deficits are not a result of WM encroachment.

Growth rate maps such as these may offer a surrogate marker and phenotypic targets for genetic and interventional studies of schizophrenia. A practically useful finding in COS was the high correlation ($R = 0.64$; $P = 0.029$) between growth rates in WM overall and functional improvement in the CGAS score. This suggests that the positive growth values may reflect a functional increase in the processing capacity of WM, perhaps because of increases in myelination and axonal conduction speed. This is further supported by our two recent observations from GM cortical thickness analyses for the COS cohort and their healthy siblings. In the healthy COS siblings ($n = 52$, 113 scans), amelioration of regional GM deficits was associated with higher global functioning (10). Similarly, in a sample of 46 COS patients, thicker cortical GM at admission positively correlated with remission status at discharge, 3–4 months after the scan (24). However, it must be conceded that the patients whose CGAS scores improve most between baseline and follow-up are typically those with greatest functional impairment at baseline, so faster growth rates predict greater recovery in terms of change rather than the absolute level of functioning at follow-up. Furthermore, the correlations assume that the trajectory of the CGAS improvement is linear, as is also assumed for WM growth, which may not be the case. Because of the limited number of time points, it is not possible to establish (or rule out) a potentially nonlinear aspect of the CGAS trajectory, and improvement in scores may have taken place in the initial period after treatment. Additional follow-up scans and cognitive assessments over larger time periods would be needed to test this. Even so, a key requirement for

Table 2. Average tissue deficits at baseline and follow-up

Region	Baseline scan		Follow-up scan		Change
	Volume deficit	*P* value	Volume deficit	*P* value	Volume deficit
White matter overall	−2.86	0.0004	−3.42	0.001	−0.56
Left hemisphere	−2.88	0.004	−3.28	0.012	−0.40
- Frontal lobe	−3.06	0.011	−3.93	0.026	−0.87
- Parietal lobe	−4.61	0.005	−5.26	0.004	−0.65
- Occipital lobe	−3.03	0.166	−3.23	0.112	−0.20
- Temporal lobe	−1.70	0.245	−2.77	0.077	−1.07
Right hemisphere	−2.85	0.0005	−3.56	0.0004	−0.71
- Frontal lobe	−5.57	0.0003	−5.84	0.0006	−0.27
- Parietal lobe	−3.95	0.045	−5.43	0.0005	−1.48
- Occipital lobe	−0.60	0.810	−1.42	0.201	−0.82
- Temporal lobe	−0.84	0.590	−0.56	0.276	0.28
Anterior cingulate region	−6.53	0.014	−7.12	0.002	−0.59
Left hemisphere	−5.65	0.014	−5.72	0.012	−0.07
Right hemisphere	−7.16	0.042	−8.11	0.001	−0.95

Percentage reductions in tissue volume are shown for COS patients relative to healthy controls, at baseline, and follow-up, along with corrected *P* values indicating significance. The degree to which the deficit increased is also shown. Negative numbers denote increasing abnormality over time.

CORRELATION OF CHANGE IN CGAS WITH TISSUE GROWTH RATE
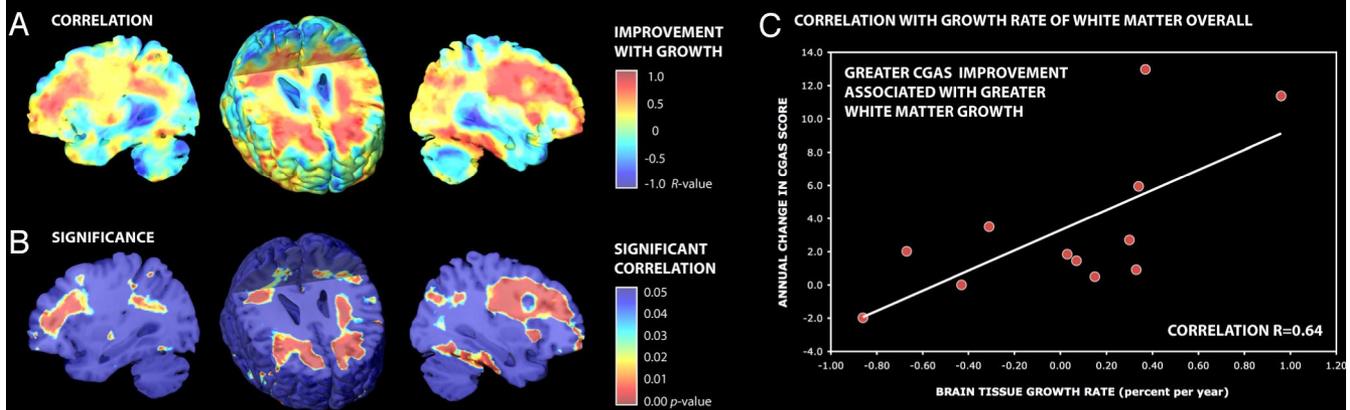
Fig. 5. Clinical correlations with tissue growth rates. The correlation between growth rates at each location in the brain and improvement on the CGAS score (follow-up minus baseline) is highly significant. (*A*) Faster growth in the frontal and parietal regions is tightly linked to recovery of function, with positive correlations exceeding 0.5 in many regions. (*B*) These linkages are highly significant (red) in the frontal WM. (*C*) The graph shows relationship between CGAS scores and overall WM growth. Three-dimensional versions of these maps are obtainable as video sequences at: http://www.loni.ucla.edu/~thompson/MOVIES/GROWTH/video.html.

image-based biomarkers of disease burden is their ability to index clinically or behaviorally relevant changes, and the WM changes hold promise as drug trial targets.

At baseline, the frontal WM already showed around 15% reduction in COS patients relative to healthy controls, and at follow-up, more of the posterior WM was reduced. This increasing deviation between COS patients and healthy controls is attributable to the silencing of growth rates in COS. The pattern of early frontal and late parietal deficits is consistent with the front-to-back developmental sequence for WM between age 3 and 15 (17). Using a similar analysis method but a different sample of scans, Hua *et al.* (14) and Chung *et al.* (25) replicated our finding of late temporo-parietal growth around the age of puberty (14, 17). As such, the progressive WM deficits could be interpreted as resulting from a failure in the normally occurring growth sequence, with increasing group differences in the regions that normally grow fastest.

The GM development in COS shows spreading deficits in the parieto-frontal direction (7), which is similar to the pattern of GM maturation (11) seen in normal development, suggesting deficits in the inhibitory controls over the normally occurring pruning process (26). In contrast, the progression of WM deficits, when groups are compared at baseline and at 5 year follow-up, appears to progress from frontal to parietal lobes. Normal WM maturation involves a process of "growth" in volume (primarily because of increased myelination), whereas the normal GM maturation process involves "loss" in GM volume. Thus, the "deficits" in WM growth in COS might also be expected to follow the same direction as the normal WM growth. A sample with a broader age span, with similar matching of scan intervals, would be needed to test this hypothesis, because it requires information on the spatial shifting of tissue changes seen with TBM and cortical mapping (27).

Much of the COS imaging literature has focused on GM changes in the cortex, hippocampus, and amgydala (6, 7, 9, 28) revealing remarkable waves of spreading abnormalities, and/or aberrant myelination in the cortex (29). There is increasing evidence of disturbed structural and functional connectivity of subcortical fiber tracts in schizophrenia as suggested by functional neuroimaging and electrophysiological studies (30–32). In AOS, magnetic resonance spectroscopy (33), DTI, and methods to establish functional connectivity (34) have shown widespread WM aberrations. Studies using voxel-based morphometry analyses have also shown abnormalities in total WM volume (35), in the superior temporal lobe (36), internal capsule (37), anterior commissure (38), and corpus

callosum (38). However, none of these cross-sectional studies provides information on growth rates as visualized in this TBM study, which also provides substrates to address the question of disconnectivity in schizophrenia.

Our findings suggest that WM maturation may be abnormal and progressive in COS, but the fact that abnormalities are not complete at psychosis onset suggests a window of opportunity, at least in principle, for treatment. It is not clear whether WM wiring or integrity is already abnormal *in utero* or whether a largely postonset deterioration in function and structure of the cortical areas is driving Wallerian changes or disruption of myelination in the fibers that innervate them. The maps of baseline differences in brain structure suggest that substantial deficits in brain structure are already present at the time of the first psychotic episode, consistent with studies of adults at high risk for schizophrenia (39). Additional twin and family studies would be needed to clarify the nature of these changes.

Some qualifications are necessary regarding these findings. Although the sample of 12 COS patients and 12 healthy controls did provide the power necessary to map group differences, because carefully matched patients and controls on age, sex, and scan interval time were selected, a larger sample would possibly also detect secondary effects of modulatory factors on growth rates (e.g., medication, sex differences, etc.). However, because growth may exhibit detectable nonlinearities over longer time spans, we preferred a design using careful matching of individuals for age and scan interval which resulted in strong statistical power for the analyses and avoided age related confounds. As with any small sample, the findings should be generalized only with caution. First, it is possible that the severely ill treatment refractory COS cohort exhibited greater departures from normal than would be typical in AOS. Second, the influence of medications on these findings cannot be ruled out because antipsychotic treatments may modulate the trajectory of cortical change in adult-onset patients (40). However, our preliminary analyses of a group of patients with atypical psychosis who had similar medication and treatment histories did not show lag in WM growth over a 2-year period (data not shown). Larger, well-matched samples would be necessary to confirm these findings.

In the near future, advances in our ability to map WM maturation should increase the processing efficiency and power of large-scale studies of COS and other developmental processes, promising to

identify new factors that affect normal and abnormal brain development in large populations.

Materials and Methods

All subjects were recruited as part of an ongoing National Institute of Mental Health study of COS and normal brain development. Twelve COS patients (6 male, 6 female) and 12 healthy controls (6 male, 6 female), who were matched for age, sex, and scan interval, were evaluated prospectively during a 5-year longitudinal study (we will refer to this as a 5-year study although strictly speaking, the mean interscan interval was 4.6 years). This sample has been analyzed for dynamic GM mapping in COS (9, 32).

COS Patients. All 12 COS patients (baseline age, 14.1 ± 0.8 yrs; follow-up age, 18.7 ± 0.9 yrs; average age 16.3 yrs; scan interval, 4.6 ± 0.3 yrs) satisfied unmodified Diagnostic and Statistical Manual of Mental Disorders (DSM) 3rd ed. revised/DSM 4th edition diagnostic criteria for schizophrenia with onset of psychotic symptoms before age 13. All patients had a history of poor response to, or intolerance of, at least two neuroleptics (treatment refractory). Patients had no other active neurological or medical conditions. Diagnosis was determined from clinical and structured interviews with the adolescents and their parents based on portions of the kiddie version of Schedule for Affective Disorders and Schizophrenia and from medical records. Psychopathologic symptoms were evaluated by means of the Scale for the Assessment of Positive Symptoms, the Scale for the Assessment of Negative Symptoms, and the CGAS (12).

Healthy Controls. Twelve healthy controls (baseline age, 13.5 ± 0.7 yrs; follow-up age, 18.0 ± 0.8 yrs; average age 15.8 yrs; scan interval, 4.6 ± 0.1 yrs) were matched with the COS patients for age, gender, social background, and height. Any neurological or psychiatric illnesses or learning disabilities were exclusionary.

MRI. All images were acquired by using a 1.5T General Electronic Signa MRI scanner located at the National Institute of Health Clinical Center (Bethesda, MD).

Three-dimensional (256 × 256 × 124 resolution), T1-weighted fast spoiled gradient echo MRI volumes were acquired longitudinally. Imaging parameters were time to echo, 5 ms; time to repeat, 24 ms; flip angle, 45°; and field of view, 24 cm. All subjects were scanned identically at baseline and follow-up. The parents or legal guardians of all subjects provided written consent for participation in this study and the subjects provided written assent.

Image Processing. All scan pairs were processed as in our longitudinal TBM studies (41, 42), and full details of the image processing steps, statistical analyses, and advantages and limitation of TBM are in the supporting information (SI) *Text*.

Briefly, follow-up scans were aligned (by using global scaling) to the same subject's baseline scan, and both were aligned to the International Consortium for Brain Mapping single subject, high-resolution brain template (HRBT) to adjust for intersubject differences in overall brain size and head alignment. For the longitudinal aspects of the study, the growth rates were computed at each point in each subject's initial scan, elastically stretching the baseline to the follow-up scan by using an elastic image registration algorithm (41). Then, to allow voxelwise statistical group analysis of local tissue growth rate maps, a second deformation of the initial scan to the HRBT was computed to elastically register each individual's annualized Jacobian map to the standard anatomical space of the HRBT. Significance maps were generated by using voxelwise statistics to assess whether the local rate of brain tissue change was significant, and whether it depended on the covariate of interest (diagnosis, clinical scores). To visualize the pattern of voxelwise significance, both R values (correlation) and p values (significance) were mapped. Omnibus significance was confirmed by using ROI-based permutation testing to provide corrected P values. As before, suprathreshold voxels were counted and compared with their null distribution ascertained from 10,000 random assignments of the covariates to the subjects.

1. Rapoport JL, Addington AM, Frangou S, Psych MR (2005) The neurodevelopmental model of schizophrenia: Update 2005. *Mol Psychiatry* 10:434–449.
2. Greenstein D, et al. (2006) Childhood onset schizophrenia: Cortical brain abnormalities as young adults. *J Child Psychol Psychiatry* 47:1003–1012.
3. Shenton ME, Dickey CC, Frumin M, McCarley RW (2001) A review of MRI findings in schizophrenia. *Schizophr Res* 49:1–52.
4. Cannon TD, et al. (2002) Cortex mapping reveals regionally specific patterns of genetic and disease-specific gray-matter deficits in twins discordant for schizophrenia. *Proc Natl Acad Sci USA* 99:3228–3233.
5. Harrison PJ, Weinberger DR (2005) Schizophrenia genes, gene expression, and neuropathology: On the matter of their convergence. *Mol Psychiatry* 10:40–68.
6. Rapoport JL, et al. (1999) Progressive cortical change during adolescence in childhood-onset schizophrenia. A longitudinal magnetic resonance imaging study. *Arch Gen Psychiatry* 56:649–654.
7. Thompson PM, et al. (2001) Mapping adolescent brain change reveals dynamic wave of accelerated gray matter loss in very early-onset schizophrenia. *Proc Natl Acad Sci USA* 98:11650–11655.
8. Rapoport JL, et al. (1997) Childhood-onset schizophrenia. Progressive ventricular change during adolescence. *Arch Gen Psychiatry* 54:897–903.
9. Nugent TF, III, et al. (2007) Dynamic mapping of hippocampal development in childhood onset schizophrenia. *Schizophr Res* 90:62–70.
10. Gogtay N, et al. (2007) Cortical brain development in nonpsychotic siblings of patients with childhood-onset schizophrenia. *Arch Gen Psychiatry* 64:772–780.
11. Gogtay N, et al. (2004) Dynamic mapping of human cortical development during childhood through early adulthood. *Proc Natl Acad Sci USA* 101:8174–8179.
12. Gogtay N, et al. (2007) Dynamic mapping of cortical development before and after the onset of pediatric bipolar illness. *J Child Psychol Psychiatry* 48:852–862.
13. Ashtari M, et al. (2007) White matter development during late adolescence in healthy males: A cross-sectional diffusion tensor imaging study. *Neuroimage* 35:501–510.
14. Hua X, et al. (2007) Detecting brain growth patterns in normal children using tensor-based morphometry *Hum Brain Mapp* [E-pub ahead of print].
15. Keller A, et al. (2003) Corpus callosum development in childhood-onset schizophrenia. *Schizophr Res* 62:105–114.
16. Kumra S, et al. (2005) White matter abnormalities in early-onset schizophrenia: A voxel-based diffusion tensor imaging study. *J Am Acad Child Adolesc Psychiatry* 44:934–941.
17. Thompson PM, et al. (2000) Growth patterns in the developing brain detected by using continuum mechanical tensor maps. *Nature* 404:190–193.
18. Chung MK, et al. (2001) A unified statistical approach to deformation-based morphometry. *Neuroimage* 14:595–606.
19. Sowell ER, et al. (2004) Longitudinal mapping of cortical thickness and brain growth in normal children. *J Neurosci* 24:8223–8231.
20. Cowell PE, Kostianovsky DJ, Gur RC, Turetsky BI, Gur RE (1996) Sex differences in neuroanatomical and clinical correlations in schizophrenia. *Am J Psychiatry* 153:799–805.
21. Narr KL, et al. (2001) Three-dimensional mapping of temporo-limbic regions and the lateral ventricles in schizophrenia: Gender effects. *Biol Psychiatry* 50:84–97.
22. Lee AD, et al. (2007) 3D pattern of brain abnormalities in Fragile X syndrome visualized using tensor-based morphometry. *Neuroimage* 34:924–938.
23. Kochunov P, et al. (2002) An optimized individual target brain in the Talairach coordinate system. *Neuroimage* 17:922–927.
24. Greenstein SK, et al. (2008) Remission status and cortical thickness in childhood-onset schizophrenia. *J Am Acad Child Adolesc Psychiatry*, in press.
25. Chung MK, et al. (2003) Deformation-based surface morphometry applied to gray matter deformation. *Neuroimage* 18:198–213.
26. Feinberg I (1982) Schizophrenia: Caused by a fault in programmed synaptic elimination during adolescence? *J Psychiatr Res* 17:319–334.
27. Thompson P, Mega MS, Vidal C, Rapoport JL, Toga AW (2001) Detecting disease-specific patterns of brain structure using cortical pattern matching and a population-based probabilistic brain atlas. *Information Processing in Medical Imaging*, eds Insana MF, Leahy RM (Springer, Berlin/Heidelberg), Vol 2082/2001, pp 488–501.
28. Vidal CN, et al. (2006) Dynamically spreading frontal and cingulate deficits mapped in adolescents with schizophrenia. *Arch Gen Psychiatry* 63:25–34.
29. Bartzokis G, et al. (2003) Dysregulated brain development in adult men with schizophrenia: A magnetic resonance imaging study. *Biol Psychiatry* 53:412–421.
30. Stephan KE, Baldeweg T, Friston KJ (2006) Synaptic plasticity and dysconnection in schizophrenia. *Biol Psychiatry* 59:929–939.
31. Davis KL, et al. (2003) White matter changes in schizophrenia: Evidence for myelin-related dysfunction. *Arch Gen Psychiatry* 60:443–456.
32. Lawrie SM, et al. (2002) Reduced frontotemporal functional connectivity in schizophrenia associated with auditory hallucinations. *Biol Psychiatry* 51:1008–1011.
33. Keshavan MS, Hogarty GE (1999) Brain maturational processes and delayed onset in schizophrenia. *Dev Psychopathol* 11:525–543.
34. Rubia K, et al. (1999) Hypofrontality in attention deficit hyperactivity disorder during higher-order motor control: A study with functional MRI. *Am J Psychiatry* 156:891–896.
35. Chua SE, et al. (2007) Cerebral grey, white matter and CSF in never-medicated, first-episode schizophrenia. *Schizophr Res* 89:12–21.
36. Witthaus H, et al. (2008) White matter abnormalities in subjects at ultra high-risk for schizophrenia and first-episode schizophrenic patients. *Schizophr Res* 102:141–149.
37. Zhou SY, et al. (2003) Decreased volume and increased asymmetry of the anterior limb of the internal capsule in patients with schizophrenia. *Biol Psychiatry* 54:427–436.
38. Hulshoff Pol HE, et al. (2004) Focal white matter density changes in schizophrenia: Reduced inter-hemispheric connectivity. *Neuroimage* 21:27–35.
39. Pantelis C, et al. (2003) Neuroanatomical abnormalities before and after onset of psychosis: A cross-sectional and longitudinal MRI comparison. *Lancet* 361:281–288.
40. Thompson PM, et al. (2008) Time-lapse mapping reveals different disease trajectories in schizophrenia depending on antipsychotic treatment. *Cerebral Cortex*, in press.
41. Leow A, et al. (2005) Inverse consistent mapping in 3D deformable image registration: Its construction and statistical properties. *Inf Process Med Imaging* 19:493–503.
42. Leow AD, et al. (2007) Statistical properties of Jacobian maps and the realization of unbiased large-deformation nonlinear image registration. *IEEE Trans Med Imaging* 26:822–832.